ISSN 0029 - 3865

CBPF-NF-003/86

PHASE SEPARATION AND DYNAMICAL SCALING IN BORATE GLASSES

by

A.F. Craievich, J.M. Sanchez[1] and
E. Williams[2]

Centro Brasileiro de Pesquisas Físicas - CBPF/CNPq
Rua Dr. Xavier Sigaud, 150
22290 - Rio de Janeiro, RJ - Brasil

[1]Henry Krumb School of Mines
Columbia University
New York, NY 10027, USA

[2]Collège de France, Paris and
L.U.R.E
Université Paris-Sud
Orsay, France

ABSTRACT

Quasi-binary B_2O_3-PbO-($A\ell_2O_3$) glasses of two different compositions and at several temperatures inside the miscibility gap were investigated using small angle x-ray scattering. Measurements were carried out using an x-ray beam from a synchrotron source in pin-hole collimation and the samples were isothermally annealed *in situ*. The experimentally determined structure function was found to be in general agreement with recently proposed scaling laws. The exponent for the time dependence of the characteristic scaling length was found to change from a minimum value of 0.24 to a maximum of 0.35 for, respectively, samples near the center and near the boundary of the miscibility gap. The time exponent for the maximum of the structure function was found to be nearly equal to three times the exponent of the characteristic length, as expected from the scaling laws. The scaling structure function changes appreciably with composition, becoming considerably sharper near the boundary of the miscibility gap.

Key-words: Dynamical scaling; Glasses; Phase separation.

I INTRODUCTION

The existence of dynamical scaling during the last stages of phase separation in binary mixtures has recently been proposed by several investigators on the basis of phenomenological and statistical models [1-3] as well as detailed computer simulations [4]. The underlying implication of dynamical scaling is that the process of phase separation is entirely controlled by a unique characteristic length R(t). The scaling hypothesis was, therefore, implicitly included in the classical coarsening theory of Lifshitz ans Slyozov. [5], although, in its present form, scaling is considerably more general. For example, analysis of data generated by different experiments and by computer simulations has led Fratzl et al. [6] to interpret the structure function as given by the product of two universal functions.

A direct consequence of dynamical scaling is that the structure function S(q,t), i.e. the Fourier transform of the composition correlation function at time t, follows a simple asymptotic behavior for large values of t. Since the time evolution of the structure function can be directly measured by small angle diffraction techniques, the theoretical evidence for dynamical scaling has also generated renewed interest in the experimental study of phase separation in binary mixtures. In particular, dynamical scaling has recently been established, at least as a very good approximation, in liquid mixtures [7-9], quasi-binary glasses [10], and binary alloys [11-13].

In order to ascertain experimentally the validity of scaling, one must determine the existence of a unique real space characteristic length R(t) and, in principle, its time dependence. Most commonly, the inverse of the characteristic length is taken to be first moment $q_1(t)$ of the structure function or, alternatively, the magnitude of the reciprocal space vector q_m corresponding to the maximum S_m of the structure function. Although both quantities provide an equally acceptable measure of the characteristic length, there are intrinsic experimental difficulties in the calculation of the moments as well as in the precise location of q_m. For example, the calculation of the first few non-divergent moments requires precise intensity measurements at large angles where the structure function is very small and thus difficult to determine accurately. On the other hand, the location of the maximum of the structure function is particularly difficult to pinpoint since q_m is sensitive to the type of collimation used for the incident beam.

In this investigation we perform a quantitative test of the scaling hyphotesis using small angle x-ray scattering (SAXS) experiments in quasi-binary borate glasses for two different compositions and several temperatures. Our investigation of two different compositions is aimed at a quantitative study of the universality of the structure function recently proposed by Fratzl et al. [6].

Among the several items that may tend to mask the scaling (or departure from scaling) of the experimentally determined structure function is the intrinsic anisotropy of crystalline alloys. This anisotropy has been documented by Hennion et

al. [11] in Al-Zn and was presumably also present in the other studies of crystalline systems [12,13]. Thus, we have chosen to study borate glasses since they are nearly ideally isotropic systems for which the time and length scales are easily accessible by means of SAXS experiments. Our experiments were carried out using high intensity x-ray radiation from a synchrotron source in pin-hole collimation, thus avoiding corrections of the measured intensity and allowing accurate intensity measurements at relatively high angles. Isothermal annealing of the glass samples was performed *in situ*.

Throughout this work we use the first moment of the structure function, $q_1(t)$, as a measure of the inverse of the real space characteristic length $R(t)$. However, scaling was also tested by means of the procedure recently outlined by Fratzl et al. [6]. This procedure is based on a global fitting of the structure function and it does not require the calculation of the first moment q_1 or the determination of q_m. We also investigated the validity of several relations implied by the scaling laws between the moments of $S(q,t)$, and between the maximum of the structure function S_m and its location q_m in reciprocal space.

The remaining sections of the paper are organized as follows. In Section II we summarize the procedures used in the preparation of the samples together with a description of the SAXS experimental setup. A brief account of the scaling laws is given in Section III, and the experimental results are presented in Section IV. A discussion of our results together with some concluding remarks are given in Section V.

II EXPERIMENTAL PROCEDURES

The glass samples were prepared from reagent grade HBO_3, PbO and Al_2O_3. The batches were melted in a platinum crucible and homogenized by stirring at 1200 C for several hours. Plate-like samples with essentially homogeneous composition were obtained directly from the melt using the splat-cooling technique. The resulting lamellae were approximately 100 μ thick, which is close to the optimum thickness for SAXS experiments.

A specially designed high temperature cell, stable within ± 1 C[14], was used for *in situ* isothermal treatment of the glass samples during SAXS measurements. The kinetics of phase separation was investigated at several temperatures for two different compositions: Composition S(B_2O_3: 80-PbO: 15-Al_2O_3:5, weight %) and composition N(B_2O_3:64-PbO:27-Al_2O_3:9) which correspond, respectively, to the classical "spinodal" and "nucleation and growth" regions as indicated in the phase diagram of Fig. 1.

The SAXS experiments were carried out using synchrotron radiation from the DCI positron storage ring at LURE (Orsay). SAXS profiles were recorded starting few seconds after the samples have been placed in the high temperature cell, during time intervales (of about 100 s) kept shorter than the times between measurements.

The station for small angle experiments at LURE provides an incoming white beam which is horizontally focussed and monochromatized by a bent, assymetrically cut germanium (111) crystal. A wavelength of 1.38 Å has been used for this investiga

tion. An ionization chamber placed before the sample monitors the intensity decay of the incoming beam. The scattering profiles are recorded by using a one-dimensional position sensitive proportional counter of resistive cathode type. Its energy resolution of 20% is enough to remove the harmonics from the beam.

Two sets of slits are used to define a pin-hole collimated beam. All the experimental data have been corrected for incident beam intensity decay, detector inhomogeneity and parasitic scattering by the standard methods. The SAXS intensities have been represented as functions of the modulus of the scattering vector q, which is equivalent to the modulus of the coordinate in reciprocal space, and it is given $q = 4\pi \operatorname{sen}\theta/\lambda$, where θ is half the scattering angle and λ the x-ray wave length.

The geometry of the incident beam cross-section (pin hole collimation) used in this work, corresponds to a resolution in reciprocal space of $\Delta q \simeq 10^{-3}\,\text{Å}^{-1}$. This geometry allowed us to avoid mathematical desmearing, which is necessary when linear collimation is used. This tends to improve the accurracy of the experimental results.

III SCALING OF THE STRUCTURE FUNCTION

An direct experimental check on theoretical models for the kinetics of phase separation may be obtained from the comparison of the predicted isotropic structure function, S(q,t), with the experimentally determined SAXS intensity I(q,t), where

q is the modulus of the scattering vector and t represents the total decomposition time after a rapid quench of the sample into a metastable or unstable region inside the misbicibility gap.

As mentioned in the Introduction, phenomenological models and computer simulation results [1-4] suggest that, for the advanced stages of phase separation, the structure function obeys a scaling law of the form:

$$S(q,t) = J(t)F[q.R(t)] \tag{1}$$

with R(t) the real space characteristic length, F(x) the scaling structure function and where the scaling factor J(t) can be shown to be proportional to $[R(t)]^d$, with d the dimensionality of the system. The relationship between the scaling factor J(t) and the characteristic length R(t) follows from the fact that the integral of the structure function S(q,t) over the entire volume in reciprocal space is time independent due to the conservation of atomic species. In general, since SAXS experiments sample only a small region in reciprocal space, a time dependence of the integrated intensity is usually observed during the early stages of a decomposition. However, the integrated SAXS intensity is expected to be time independent during the late stages of phase separation for which the final equilibrium transformed volume fraction has essentially been reached.

It is convenient to introduce the moments Q_n and the normalized moments q_n of the structure function defined by:

$$Q_n(t) = \int_0^\infty S(q,t)q^n dq \tag{2}$$

and

$$q_n(t) = Q_n(t)/Q_o(t) \tag{3}$$

With $J(t) \propto [R(t)]^d$, as required by the conservation of integrated intensity, the scaling relation (1) implies:

$$Q_n(t) = [R(t)]^{(d-n-1)} F_n \tag{4}$$

$$q_n(t) = [R(t)]^{-n} f_n \tag{5}$$

where the time independent constants F_n and f_n are, respectively, unnormalized and normalized moments of the scaling function F(x) and are defined by equations similar to (2) and (3).

The asymptotic behavior of the characteristic length may be described by:

$$R(t) \propto t^a \tag{6}$$

with the exponent a being dependent upon the microscopic mechanism of particle growth [1-4]. For example, Stauffer and Binder [1] have shown that the exponent a varies from 1/(d+3) when the controlling growth process is that of cluster coagulation to 1/d for the classical diffusion growth mechanism of Lifshitz and Slyozov [5]. Computer simulations as

well as recent experimental results in alloy systems [4,11-13] appear to confirm the predictions of Stauffer and Binder.

Equations (1) and (6) imply that the maximum of the structure function $S_m = S(q_m,t)$, evolves with time as:

$$S_m \propto t^{a'} \tag{7}$$

with $a' = 3a$. This particular relation between a and a', together with the time independence of the second moment Q_2 of the structure function, are sensitive tests on whether or not the asymptotic scaling behavior of $S(q,t)$ has indeed been reached. Some of the reported experimental data aimed at confirming the validity of scaling, however do not reproduce the expected relation $a' = 3a$ [11,13].

Besides precise measurements of the SAXS intensity itself, we may also determine accurately the first ans second moments $Q_1'(t)$ and $Q_2'(t)$ of $I(q,t)$. Since SAXS intensity measurements are carried out in arbitrary units, these moments differ from those of the structure function $S(q,t)$ by a time independent factor. On the other hand, the normalized moments $q_1(t)$ and $q_2(t)$ may be obtained directly using $I(q,t)$ in Eqs. (2) and (3). With this in mind, we have chosen the following relations, derived from Eqs. (1)-(7), in order to test the validity of the scaling hypothesis:

$$q_1(t) \propto t^{-a} \tag{8}$$

$$I_m \propto t^{a'} \tag{9}$$

$$q_2(t) \propto [q_1(t)]^2 \tag{10}$$

$$Q_0'(t) \propto [q.(t)]^{-2} \tag{11}$$

$$Q_1'(t) \propto [q_1(t)]^{-1} \tag{12}$$

$$Q_2' \propto \text{constant} \tag{13}$$

where I_m denote the maximum of the SAXS intensity $I(q_m^{'},t)$.

IV EXPERIMENTAL RESULTS

The time evolution of the SAXS intensity was determined for samples of composition S during *in situ* isothermal heat treatment at 460 C, 470 C and 480 C. Figures 2(a) and 2(b) show the measured intensity in arbitrary units for 460 C and 480 C, respectively, and several times. For this composition and temperatures, the system lies deep inside the classical spinodal region of the miscibility gap (Fig. 1). SAXS curves were also obtained from samples having the composition N and treated isothermally at 480 C, 490 C and 500 C for different lengths of time. In this case, the system is located close to the boundary of the miscibility gap (Fig. 1) where, according to the classical theory, decomposition proceeds by a "nucleation and growth" mechanism. The evolution of the SAXS curves for com

position N at 480 C and 500 C are shown, respectively, in Fig. 3(a) and 3(b).

Plots of the normalized first moment $q_1(t)$ versus t are shown in Fig. 4(a) for samples of composition S and three different temperatures (460 C, 470 C and 480 C). Figure 4(b) shows the same plots for samples of composition N at 480 C, 490 C and 500 C. As seen in the figures, the behavior predicted by Eq. (8) is closely obeyed. For the relatively narrow temperature range investigated, the exponents do not change appreciably with temperature, although they show a definite tendency to increase as we move from composition S at the center to composition N near the boundary of the miscibility gap.

The time evolution of the maximum of the SAXS intensity is shown in Figures 5(a) and 5(b) for, respectively, compositions S ans N. In all cases it is seen that the exponents a' are very closely equal to three times the corresponding exponents a shown in Table I. As mentioned in the last section, this behavior is expected from the conservation of integrated intensity during the last stages of decomposition.

The general validity of Eqs. (10) to (13) is demonstrated in Fig. 6(a) for composition S and in Fig. 6(b) for composition N. In these figures, we have plotted the moments $Q_o(t)/Q_o(t_f)$, $Q_1(t)/Q_1(t_f)$, $Q_2(t)/Q_2(t_f)$ and $q_2(t)/q_2(t_f)$, versus $q_1(t)/q_1(t_f)$, where t_f stands for the longest time investigated at each temperature and composition. The behavior predicted by Eqs. (10)-(13), indicated by the solid lines in Fig. 6, is closely followed by all the studied glass samples. In particular the second moment $Q_2(t)$ is essentially time in-

dependent. Fittings which are similar to those shown in Fig. 6 were observed for the other temperatures.

Figures 7(a) and 7(b) show plots of the ratio q_2/q_1^2 as a function of time for compositions S and N, respectively, and for all temperatures investigated. In the scaling regime, this parameter is characteristic of the scaling function itself and it equals f_2/f_1^2 (see Eq. 5).

Finally, the scaling behavior of the experimental structure function can be seen in Fig. 8 for composition S at 460 and 480 C in Fig. 9 for composition N at 480 and 500 C. In these figures we plot $[q_1(t)]^3 I(q,t)/Q_2$ versus $q/q_1(t)$. The approximately constant normalization factor Q_2 is introduced since all intensity measurements were carried out in arbitrary units. It should be noted that with this normalization factor, the scaling function F(x) is such that its second moment F_2 is equal to 1. As expected, the scattering curves corresponding to the very early stages do not follow the asymptotic scaling behavior. This deviation from the scaling law for small values of the can also be inferred, particularly for composition N, from the lack of constancy of q_2/q_1^2 seen in Fig. 7.

No significant differences between the scaling function F(x) was detected for different temperatures at the same composition. However, appreciable changes are seen from one composition to the other. In Table I three parameters that characterize semiquantitatively the scaling function are given. These are the maximum F_m, the width at half maximum Δ and the position of the maximum x_m. We see from Table I that F(x) becomes considerably sharper near the boundary of the misci-

bility gap, although the ratio of normalized moments f_2/f_1^2, shown in the sixth column of the table, remain essentially constant with temperature and composition.

V DISCUSSION AND CONCLUSIONS

We have found general agreement between the SAXS experimental results and the predictions of the statistical theories on the dynamics of phase separation for all glasses investigated, The scaling laws, and in particular Eqs. (10)-(13) are closely obeyed during the late stages of decomposition. An important experimental criterion for establishing "late stages" is the time independence of q_2/q_1^2. As seen in Fig. 7, scaling is reached relatively early in the decomposition process for samples of composition S, whereas for samples of composition N the scaling regime has apparently been reached only for the longest times measured. The plots of Fig. 7 are only meaningful to the extent that the first few moments of the SAXS intensity may be calculated accurately. In this regard, the experimental verification of the conservation of the integrated intensity, i.e. constancy of Q_2, plays a key role (see Fig. 6). Although the integrated intensity should be strictly conserved at all times, SAXS measurements can only be performed within a "window" in reciprocal space. Thus, for very early stages, the important contribution *of short-range correlations (large values of q) to the* experimental structure function are not included, which re-

sults in the time dependence of Q_2. However, once Q_2 reaches a constant value with time, one is confident that all the relevant information in the structure function is contained in $I(q,t)$. Clearly, in those cases for which the integrated intensity is seen to change with time, a more appropriate test of scaling would be the procedure proposed by Fratzl et al. [6]. For our data, however, the determination of the characteristic length by calculation of q_1 or by the graphical procedure of Fratzl et al. produce the same results.

An additional consistency check on the analysis of the experimental data is the expected relation $a' = 3a$, where $\underline{a}$ and $\underline{a}'$ are, respectively, the time exponents defined by Eqs. (8) and (9). As seen in Table I this relation is obeyed by the borate glasses for all temperatures and compositions. The relation $a' = 3a$ has not been observed in some of the metallic systems studied in the past [11,13], although the reason is most likely due to data analysis (including perhaps crystal anisotropy) than to a violation of the scaling laws.

Concerning the time exponent of the characteristic length, we obtain average values of $a = 0.25$ for composition S and $a = 0.31$ for composition N. Thus, at least qualitatively, our results appear to confirm the predictions of Stauffer and Binder [1] of a cross-over between a low temperature cluster coagulation mechanism near the center of the miscibility gap, with exponent $a = 1/(d+3)$, and the classical particle coarsening process of Lifshitz and Slyozov with exponent $a = 1/d$ near the boundary of the gap. The experimental exponents are also in good quantitative agreement with the computer simulations of

Marro et al. [4] who reported values of a ranging from 0.2 near the center to approximately 0.3 near the boundary of the miscibility gap.

The experimental scaling function F(x) shows a dependence with composition: as we move from the center to the boundary of the miscibility gap, the maximum F_m increases, it shifts to slightly larger values of x, and the width at half-maximum Δ decreases significantly (see Table I). This particular behavior of F(x) is opposite to that predicted be the model of Rikvold and Gunton [16], Furukawa [2] and the computer simulations [4]. Although different normalization schemes are used by different authors (in our case we use the second moment F_2 equal to 1), the theoretical models and simulations predict, nevertheless, a sharper scaling function near the center of the gap.

Significantly, recent work on Fe-Cr by Katano and Iizumi [13] has shown that, for the same system with composition near the center of the miscibility gap, the characteristic length exponent changes with time from a value of 0.2 characteristic of a coagulation mechanism, to 0.33 as expected from a diffusion controlled process. This cross-over in the exponent a has also been documented by Forouhi [12] in Al-Mg-Zn alloys. Concurrent with this apparent change in particle growth mechanism, Katano and Iizumi report a pronounced change in the shape of the scaling functions: F(x) becomes sharper (more peaked) during the very late stages for which the characteristic length exponent is close to 0.33. Thus, the experiments in Fe-Cr together with our results in glasses seem to indicate that the

shape of the scaling function is intimately related to the underlying growth mechanism.

In conclusion, our SAXS investigation of phase separation in glasses, performed under particularly favorable conditions (pin-hole collimation and *in situ* heat treatment), is in quantitative agreement with statistical theories and the scaling hypothesis. The results concerning the evolution of the structure function for different compositions and temperature agree well with the computer simulations of Lebowitz and co-workers. Changes in shape of the experimental scaling function with composition do not conform to the predictions of the various theoretical models available. The evidence points towards a correlation between the shape of F(x) and the mechanism of particle growth, at least to the extent that the latter is accurately reflected in the value of the characteristic length exponent a. Further experimental and theoretical work is clearly needed in order to elucidate this point.

ACKNOWLEDGEMENTS

We wish to thank E.D. Zanotto for collaboration in preparing the glass samples and S. Bras for assistance in using the position sensitive detector. One of us (AFC) acknowledges the staff of LURE for hospitality during the initial stages of this investigation.

FIGURE CAPTIONS

Figure 1: Miscibility gap for the quasi-binary B_2O_3-PbO-$A\ell_2O_3$ glass system, from Ref. 15. The continuous line is the binodal and the dashed line is the classical spinodal. The bars S and N indicate the compositions and temperature domains corresponding to the samples studied in this work.

Figure 2: Time evolution of SAXS intensity (in arbitrary units) for samples of composition S at 460 C (a) heat treated for increasing times [min]: A) 150, B) 6.55, C) 11.33, D) 18.08, E) 21.00, F) 25.63, G) 37.33, H) 46.87, I) 67.08, J) 78.00 and at 480 C (b) heat-treated for times [min]: A) 4.43, B) 7.20, C) 10.67, D) 15.00, E) 22.00.

Figure 3: Time evolution of SAXS intensity (in arbitrary units) for samples of compositions N at 480 C (a) heat treated for the following times [min] A) 10.83, B) 12.22, C) 17.00, D) 23.00, E) 29.67, F) 35.83, G) 43.83, H) 54.00, I) 62.67 and at 500 C (b) heat treated for the following times [min]: A) 1.67, B) 3.05, C) 4.50, D) 6.33, E) 7.50, F) 9.33, G) 11.00, H) 13.50, I) 16.00, J) 19.50, K) 24.00, L) 30.00.

Figure 4: Time dependence of the inverse characteristic length q_1 corresponding to composition S (a) and N (b) at the various indicated temperatures.

Figure 5: Time dependence of the maximum of the SAXS intensity corresponding to compositions S (a) and N (b) at the several indicated temperatures.

Figure 6: Dependence on the inverse characteristic length $q_1(t)$ of the moments $Q_n(t)$ $(n = 0,1,2)$ and the normalized second moment $q_2(t)$ of the structure function for composition S at 460C. All moments are normalized to the corresponding value t_r at the longest aging time.

Figure 7: Time dependence of the ratio q_2/q_1^2 for compositions S (a) and N (b) at several temperatures.

Figure 8: Scaling of the structure function for composition S at 460 C (a) and 480 C (b).

Figure 9: Scaling of the structure function for composition N at 480 C (a) and 500 C (b).

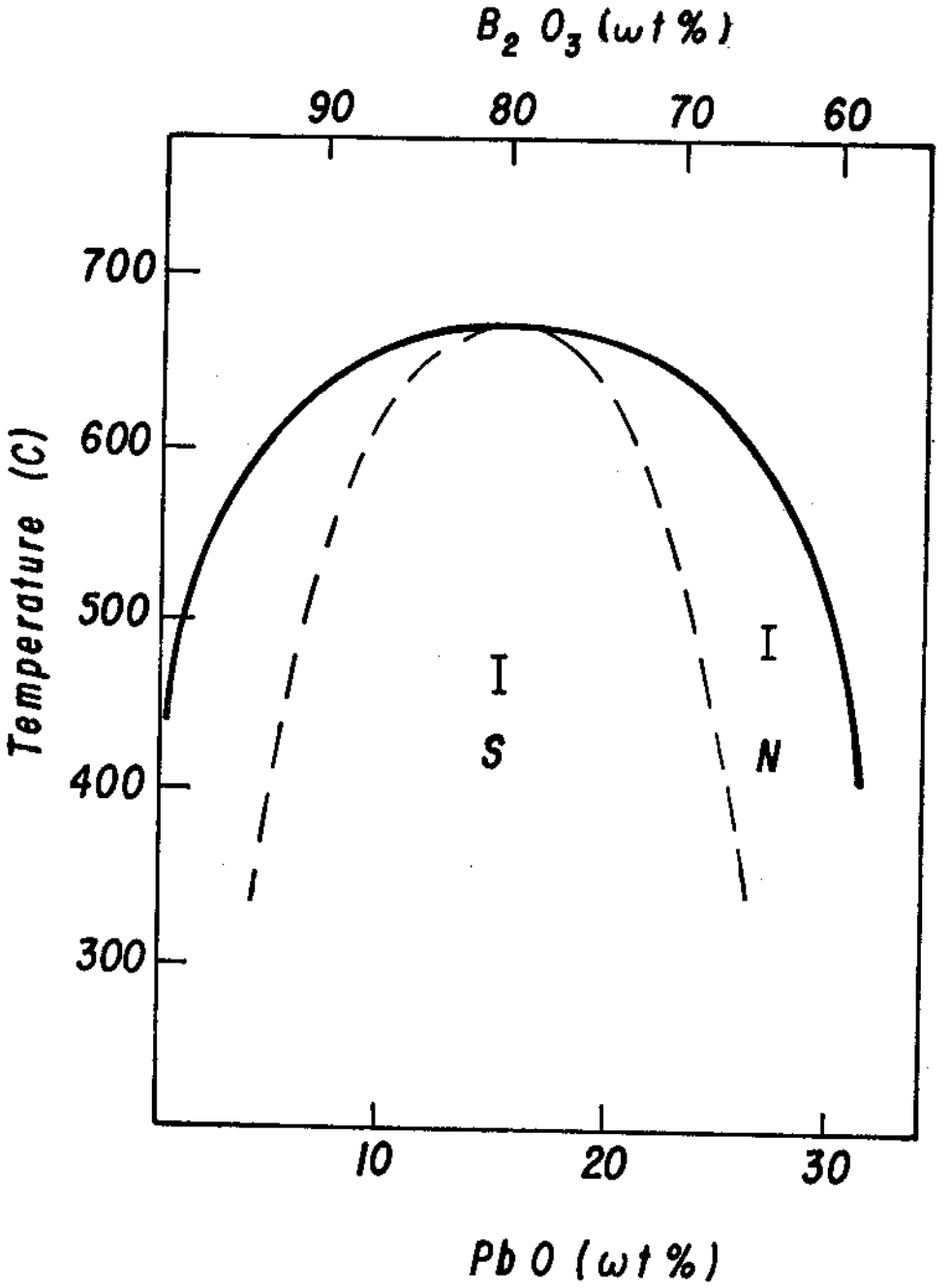
B_2O_3 (wt %)
90
80
70
60
700
600
500
400
300
Temperature (C)
I
S
I
N
10
20
30
PbO (wt %)

FIG. 1

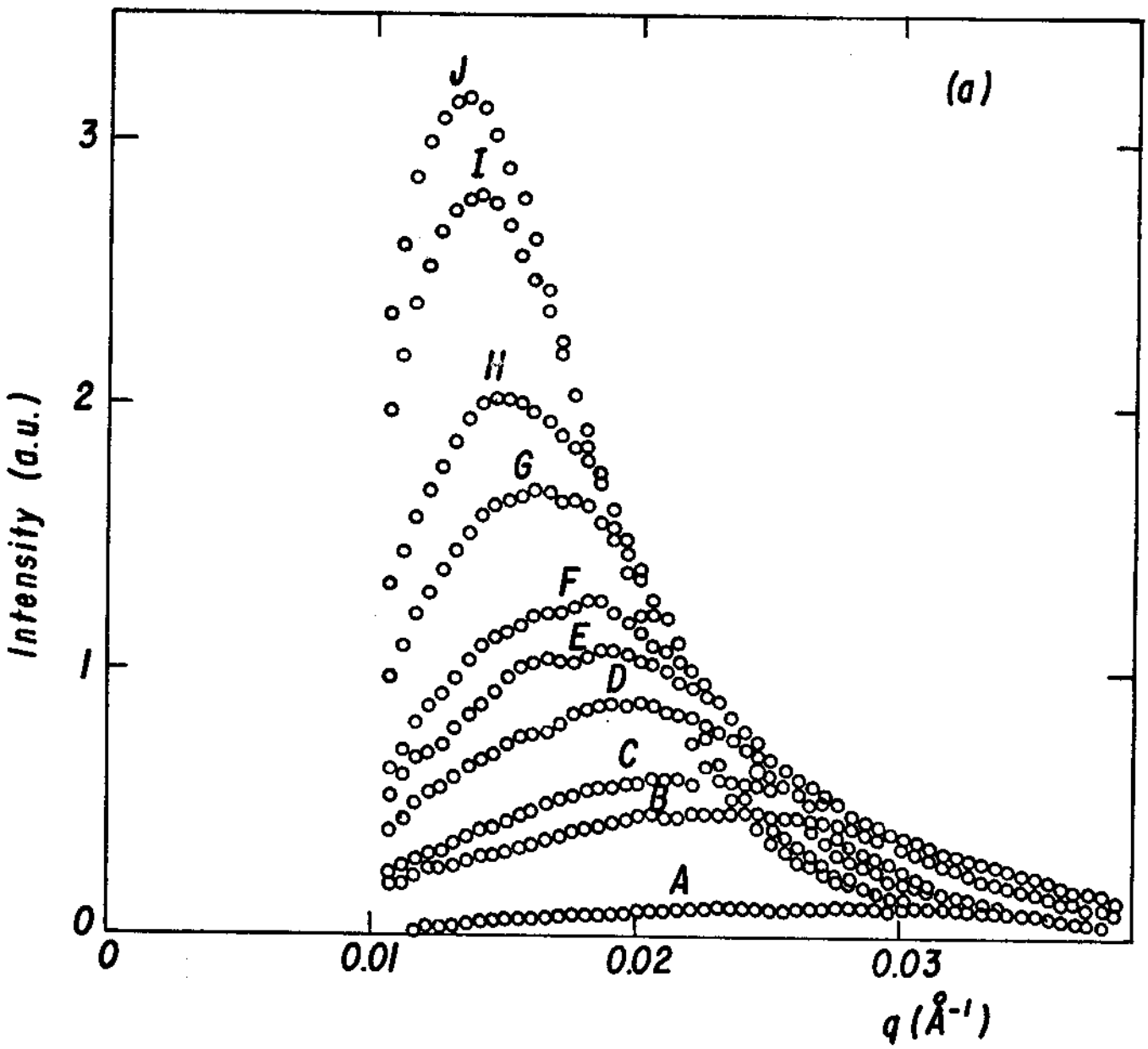

FIG. 2a

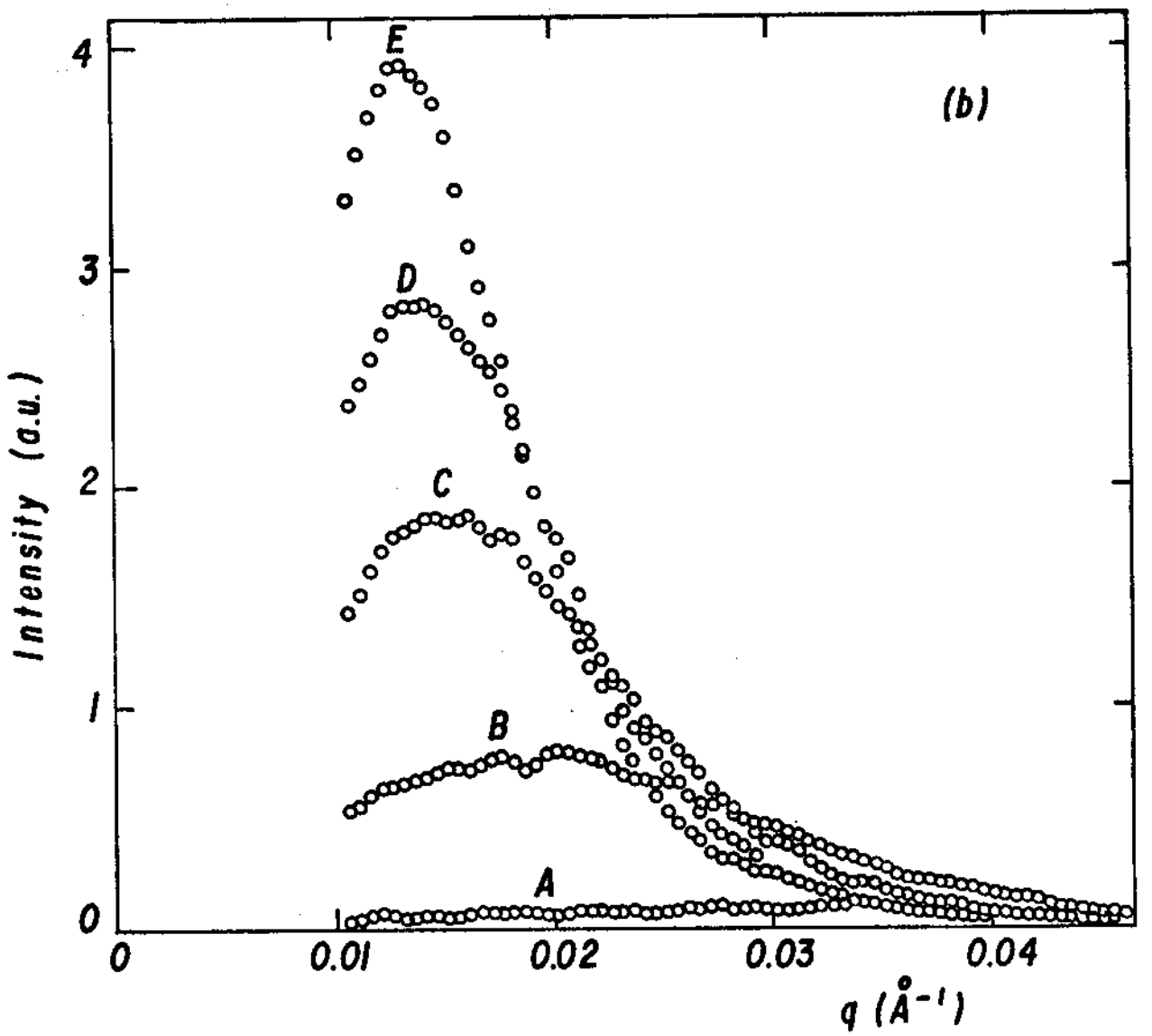

FIG. 2b

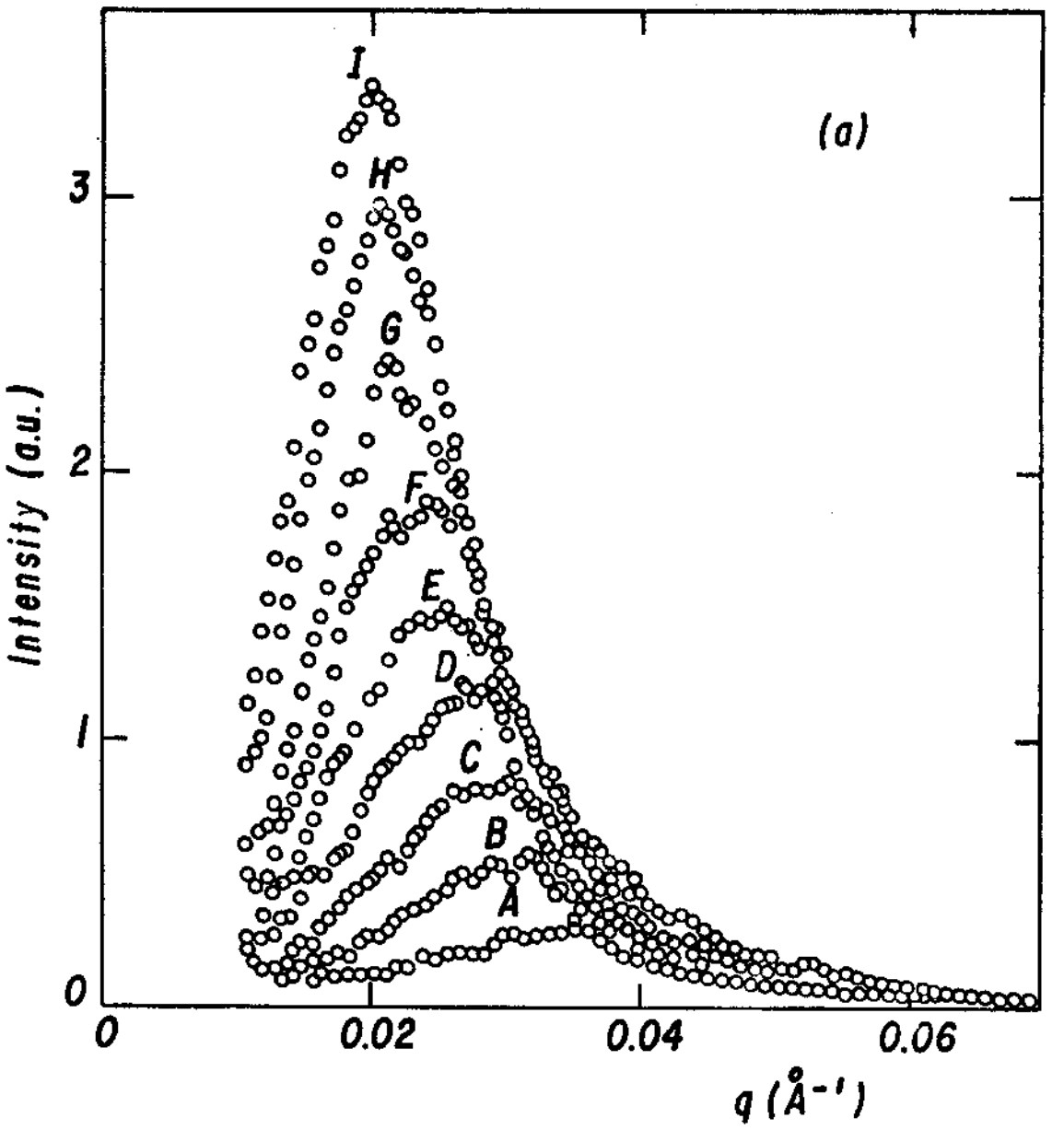

FIG. 3a

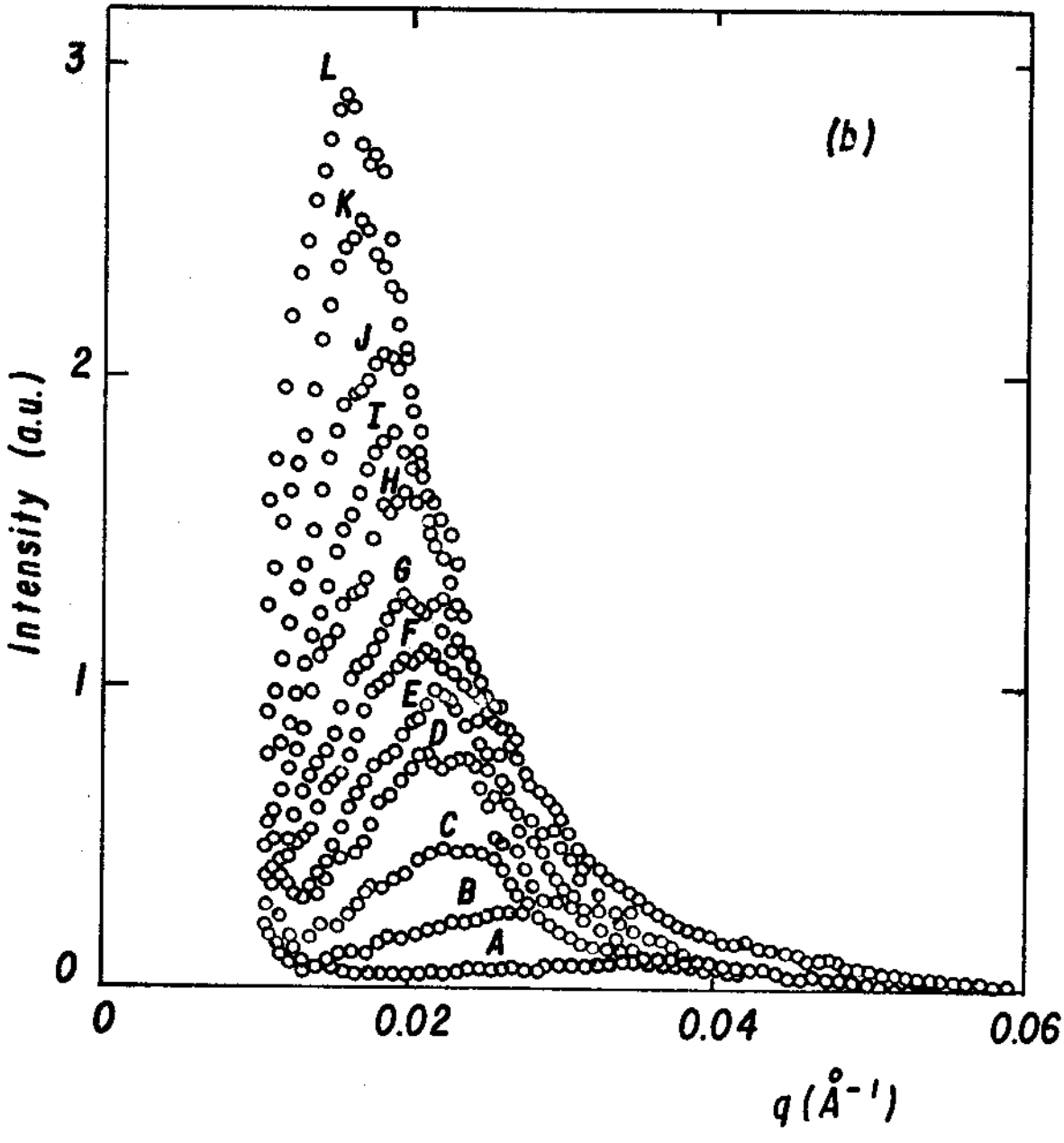

FIG. 3b

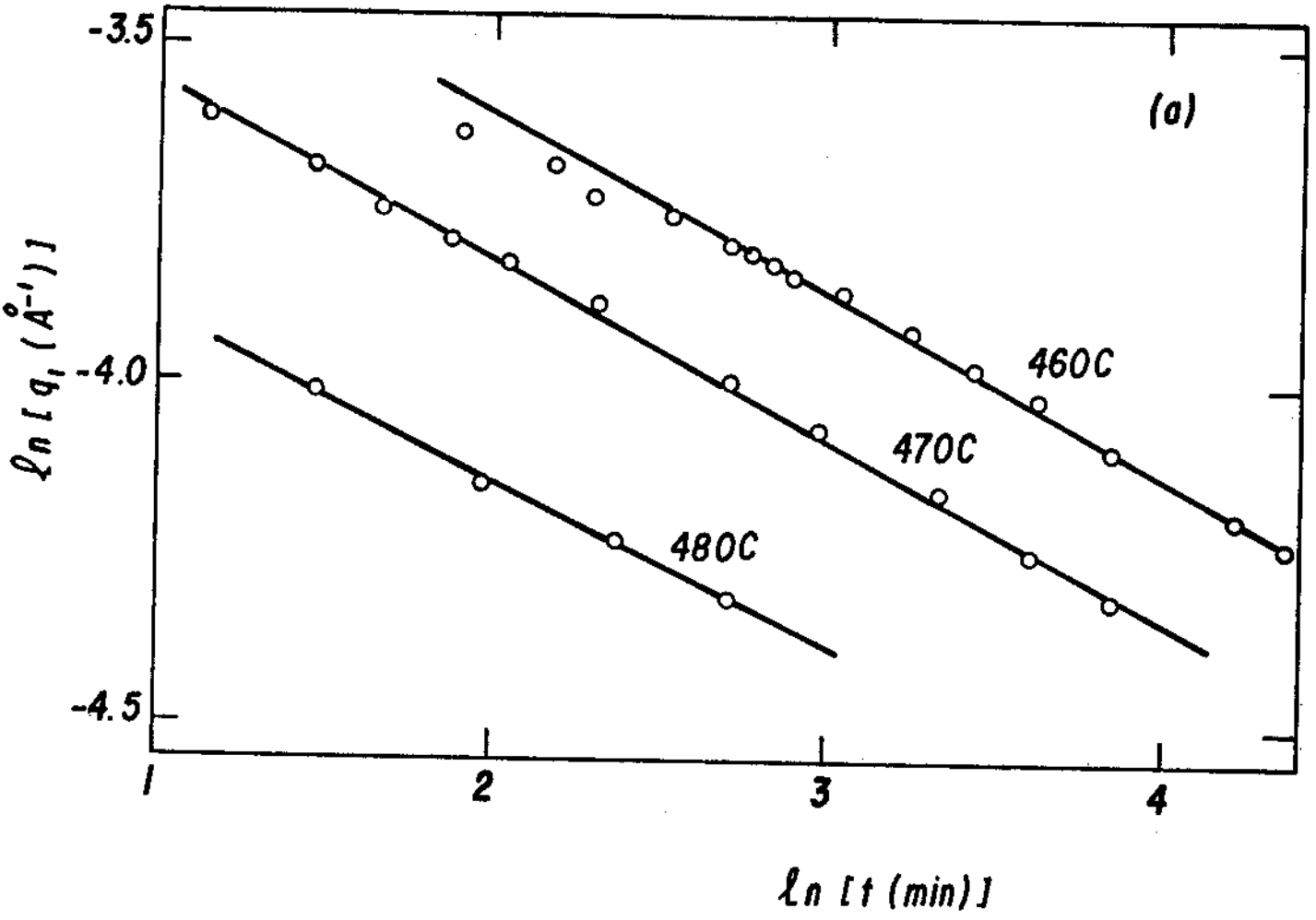

FIG. 4a

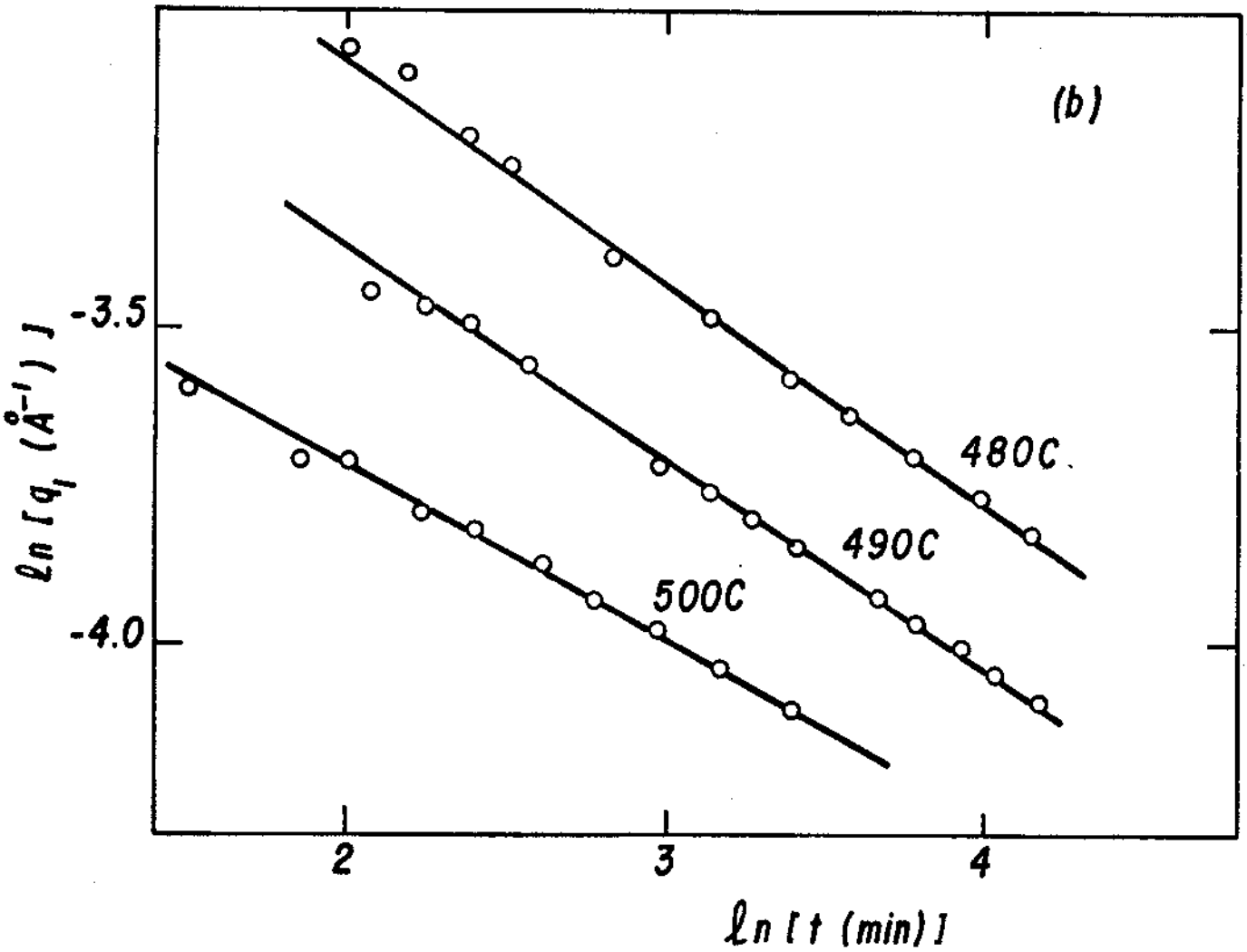

FIG. 4b

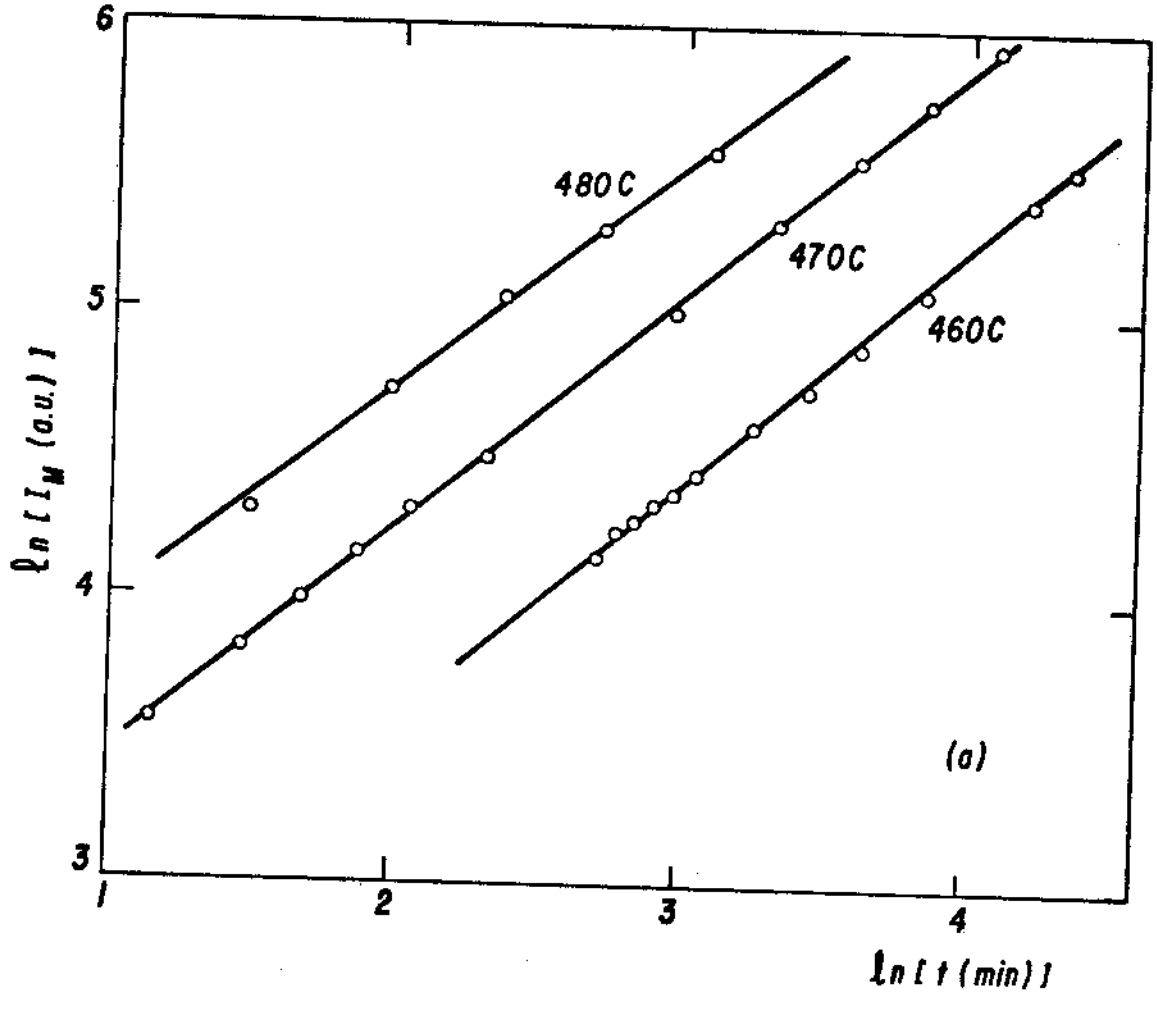

FIG. 5a

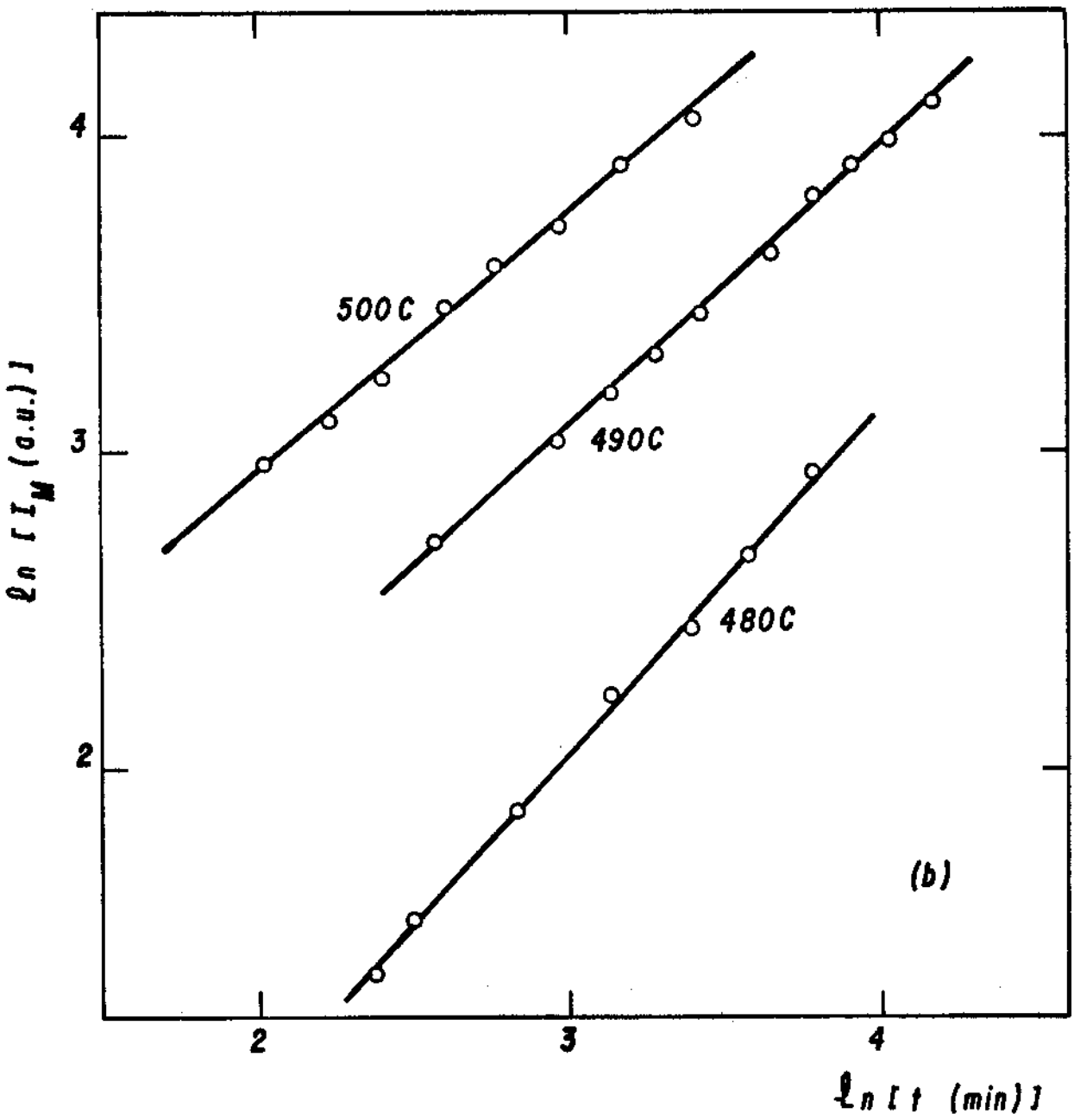

FIG. 5b

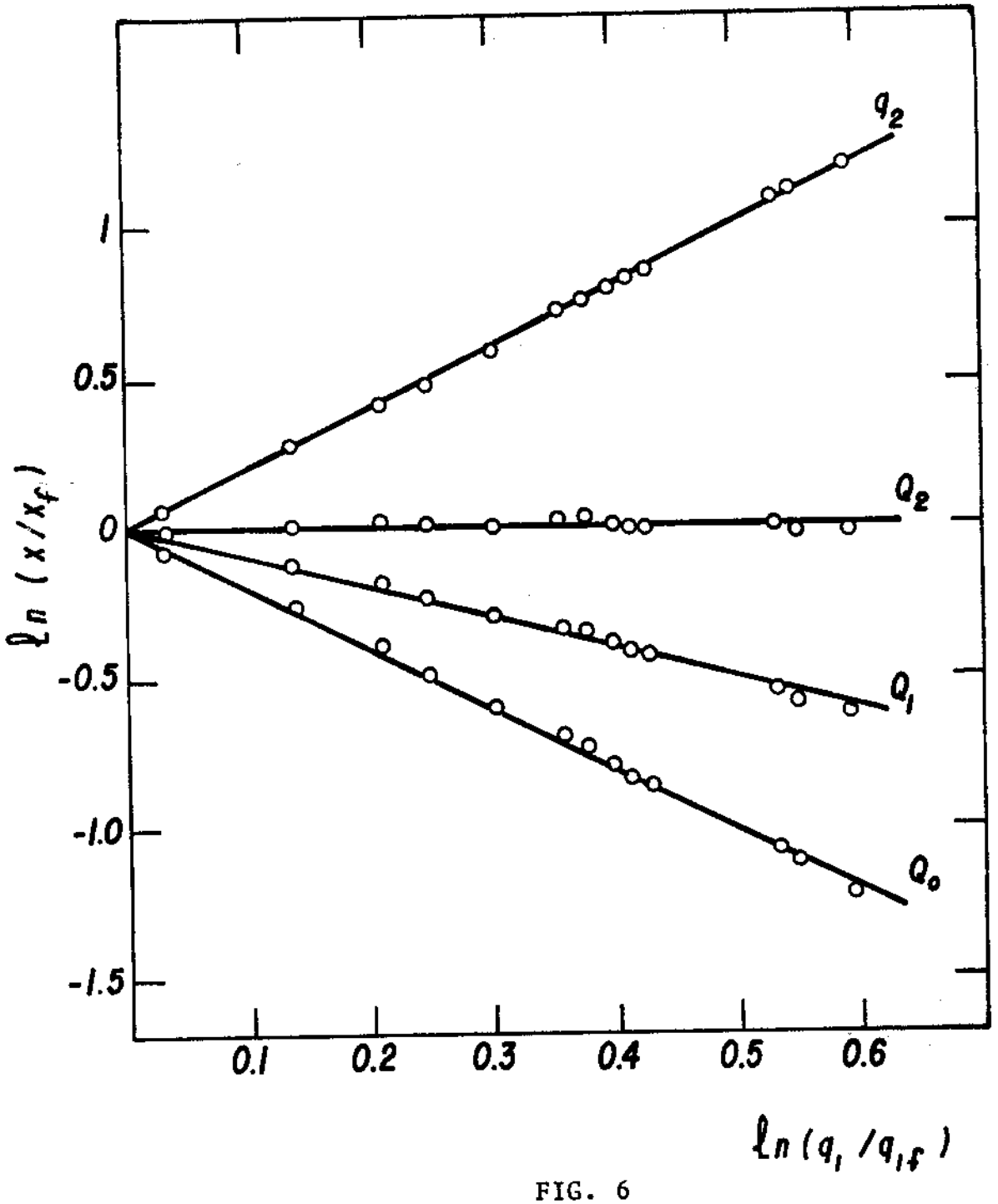

FIG. 6

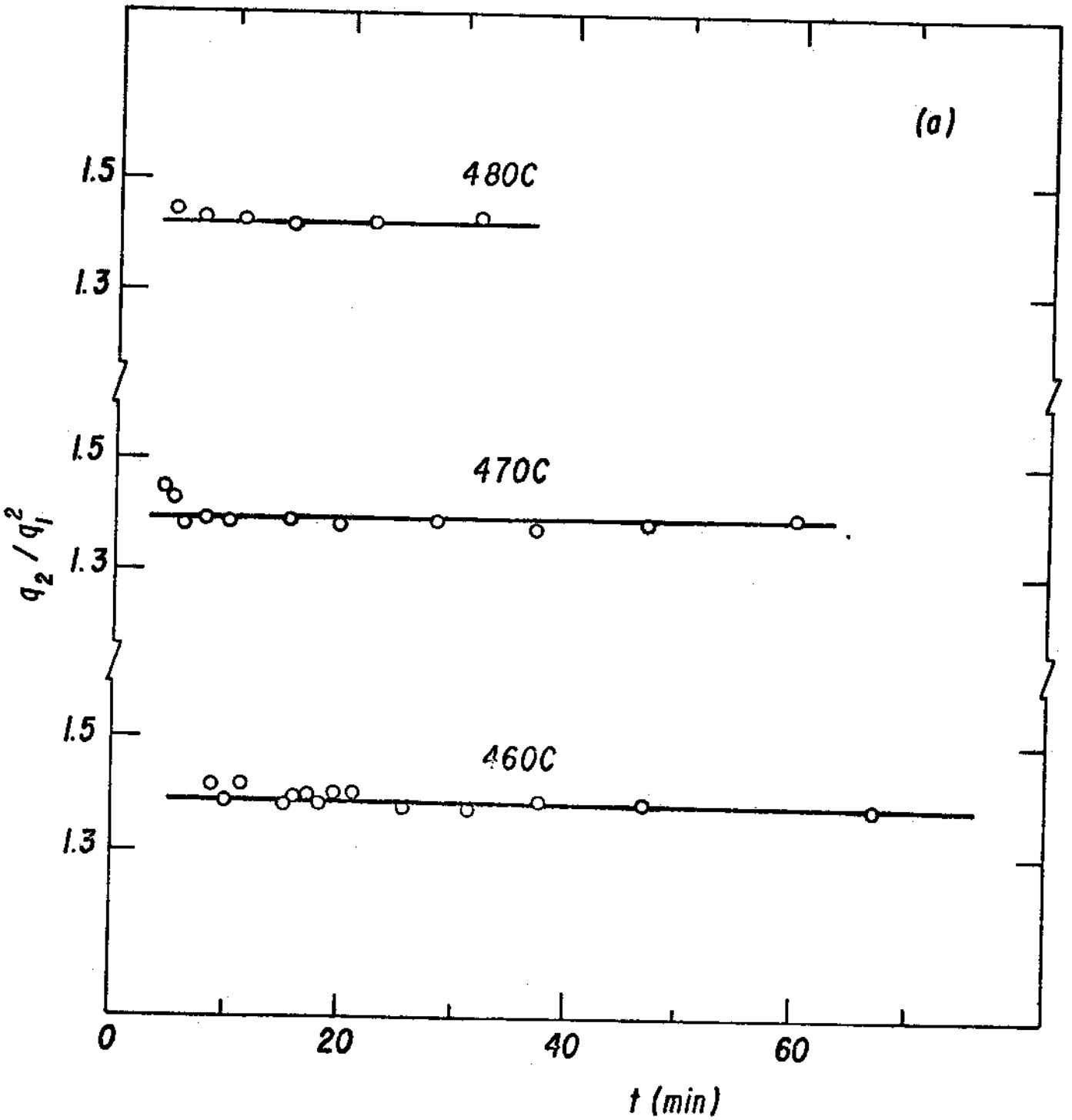

FIG. 7a

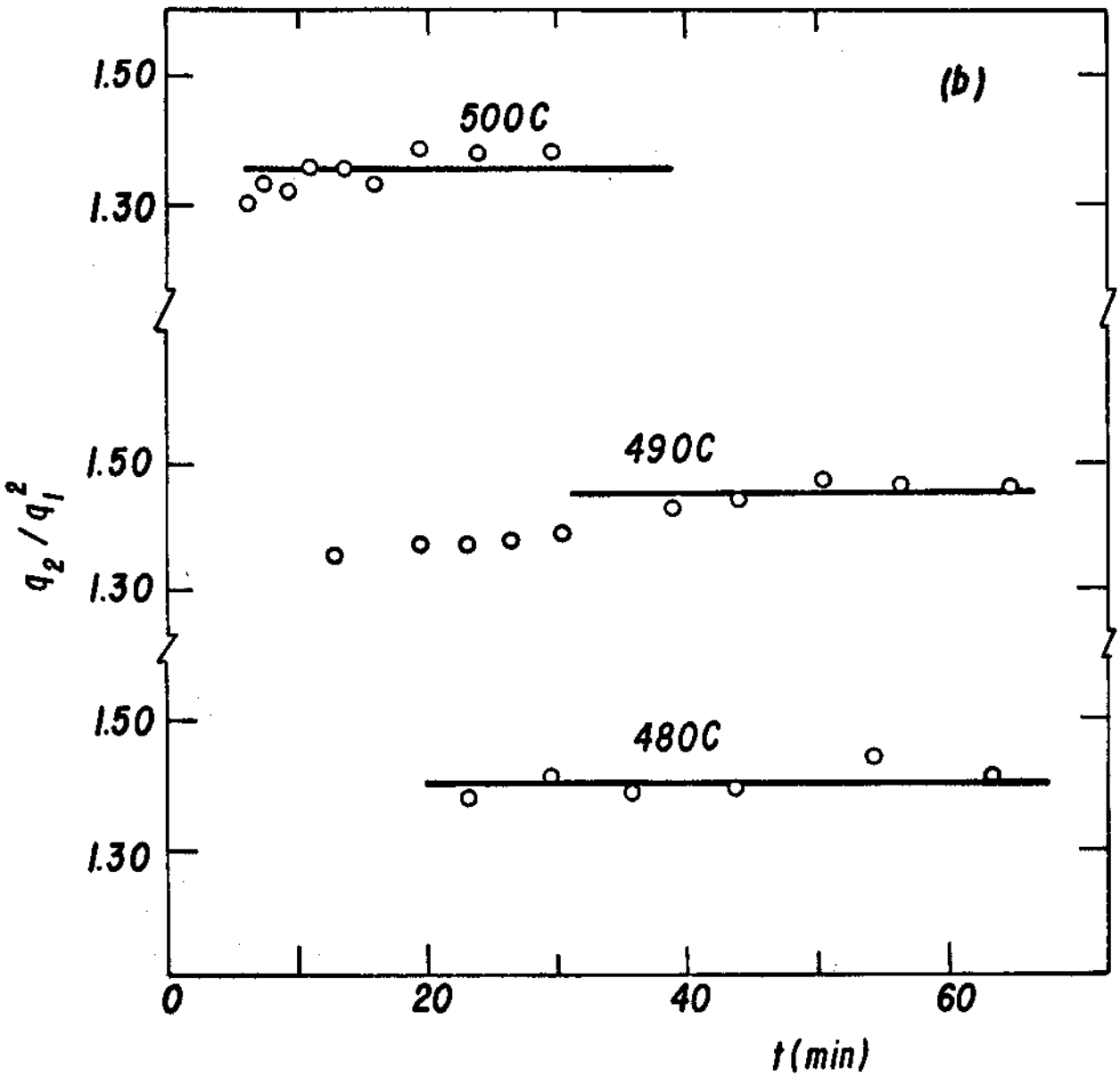

FIG. 7b

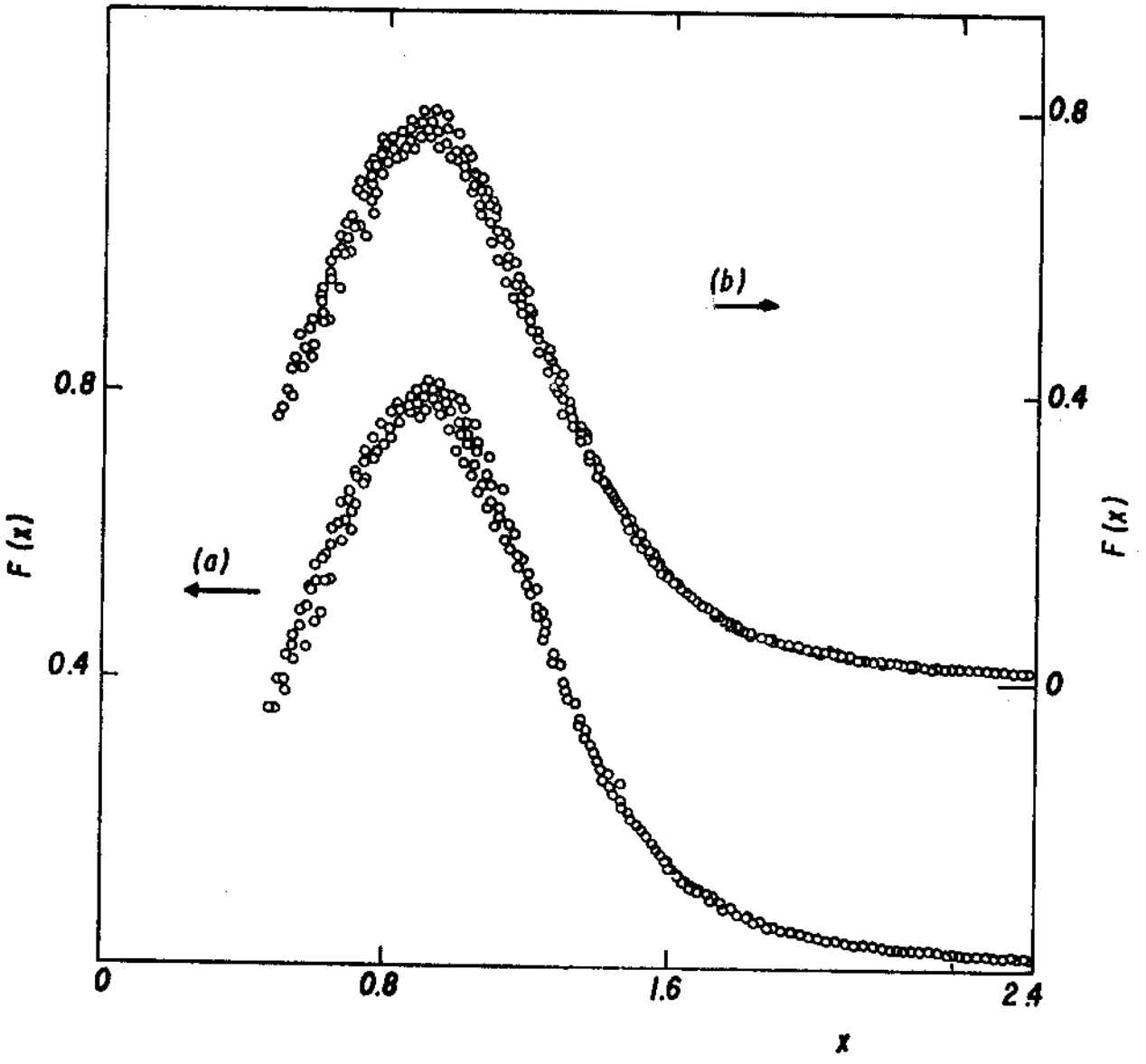

FIG. 8

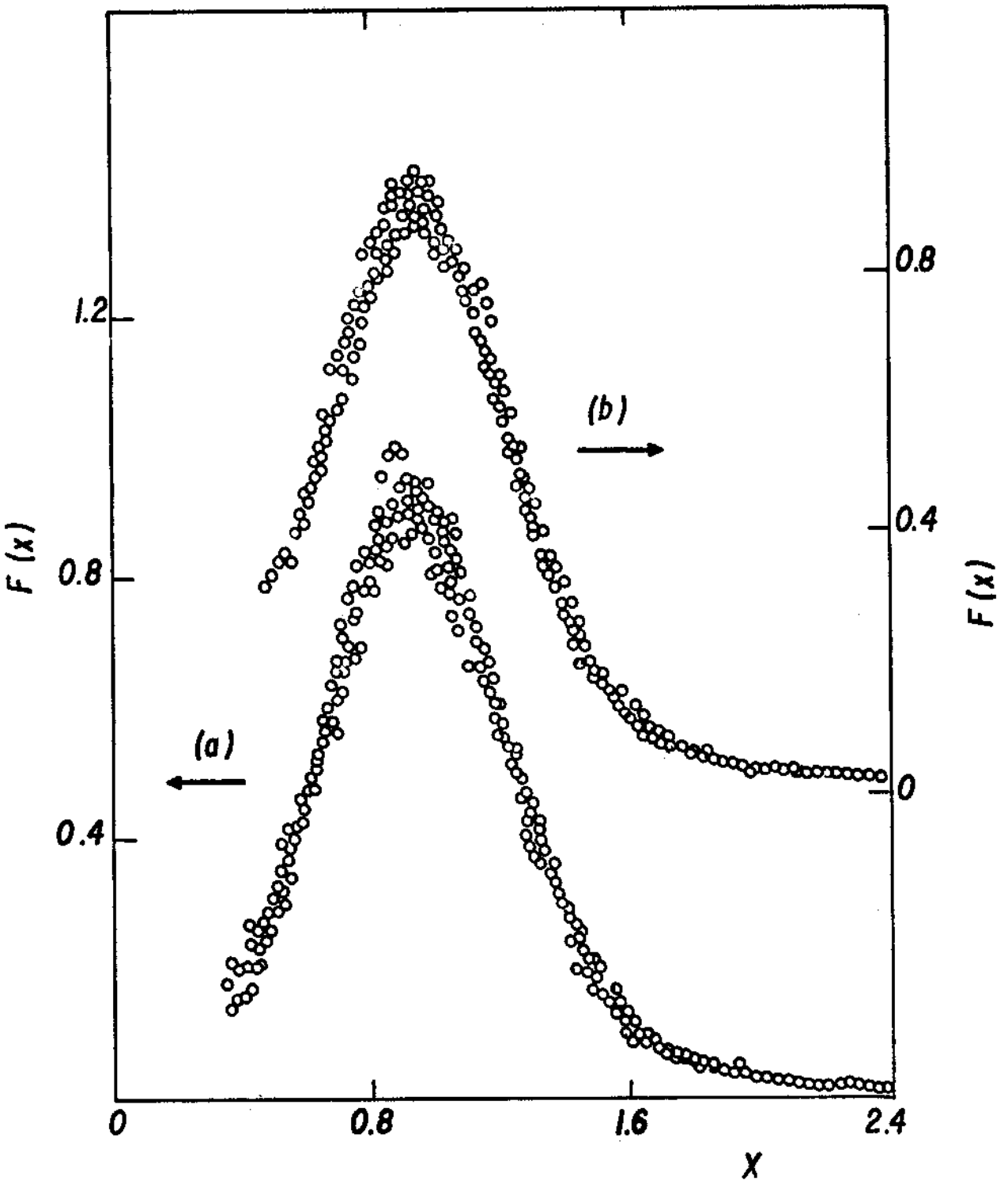

FIG. 9

TABLE I

Scaling parameters for samples with weight % compositions B_2O_3:80 - PbO:15 - $A\ell_2O_3$:5 (S) and B_2O_3: 64 - PbO:27 - $A\ell_3O_2$:9 (N). F_m, x_m and Δ indicate the maximum, the position of the maximum and the half- maximum width, respectively, of the experimental scaling function.

Sample	T[c]	q_2/q_1^2	a	a'	3a	F_m	x_m	Δ
S	460	1.39	0.26	0.83	0.78	0.77	0.90	0.80
S	470	1.40	0.26	0.81	0.78	0.79	0.90	0.80
S	480	1.42	0.24	0.77	0.72	0.78	0.90	0.80
N	480	1.41	0.35	1.10	1.05	0.92	0.94	0.68
N	490	1.45	0.32	0.90	0.96	0.92	0.94	0.68
N	500	1.38	0.27	0.84	0.81	0.92	0.94	0.68

REFERENCES

1. K. Binder and D. Stauffer, Phys. Rev. Lett. 33, 1006 (1974); K. Binder, Phys. Rev. B 15, 4425 (1977).
2. H. Furukawa, Phys. Rev. Lett. 43, 136 (1979); H. Furukawa, Phys. Rev. A 23, 1535 (1981).
3. E.D. Siggia, Phys. Rev. A 20, 595 (1979).
4. A.B. Bortz, M.H. Kalos, J.L. Lebowitz, and M.H. Zendejas, Phys. Rev. B 10, 535 (1974); J. Marro, A.B. Bortz, M.H. Kalos and J.L. Lebowitz, Phys. Rev. B12 2000 (1975); M. Rao, M. H. Kalos, J.L. Lebowitz, and J. Marro, Phys. Rev. b 13, 4328 (1976); J. Marro, J.L. Lebowitz and M.H. Kalos, Phys. Rev. Lett. 43, 282 (1979); J.L. Lebowitz, J. Marro and M. H. Kalos, Acta Metall. 30, 297 (1982).
5. I.M. Lifshitz and V.V. Slyozov, J. Phys. Chem. Solids 19, 35 (1961).
6. P. Fratzl, J.L. Lebowitz, J. Marro and M.H. Kalos, Acta Metall. 31, 1849 (1983).
7. C.M. Knobler and N.C. Wong, J. Phys. Chem. 85, 1972 (1981).
8. Y.C. Chou and W.I. Goldburg, Phys. Rev. A 23, 858 (1981).
9. D.N. Sinha and J.K. Hoffer, Physica (Utrecht) 107B+C, 155 (1981).
10. A.F. Craievich and J.M. Sanchez, Phys. Rev. Lett. 47, 1308 (1981).
11. M. Hennion, D. Ronzaud and P. Guyot, Acta Metall. 30, 599 (1982).
12. A.R. Forouhi, Doctoral Dissertation, University of California, Berkeley, 1982 (unpublished).

13. S. Katano and M. Iizumi, Phys. Rev. Lett. 52, 835 (1984);
S. Katano and M. Iizumi, Physica (Utrecht), 120B, 392 (1983).

14. A. Craievich, J. Appl. Cryst. 7, 634 (1974).

15. J. Zarzycki and F. Naudin, J. Non-Cryst. Solids 1, 215 (1969).

16. P.A. Rikvold and J.D. Gunton, Phys. Rev. Lett. 49, 1223 (1982).